

Can the angular scale of cosmic homogeneity be used as a cosmological test?

Xiaoyun Shao^{1,*}, Rodrigo S. Gonçalves^{1,2,†}, Carlos A. P. Bengaly^{1,‡},
Uendert Andrade^{3,§}, Gabriela C. Carvalho^{4,¶} and Jailson Alcaniz^{1,**}

¹*Observatório Nacional, 20921-400, Rio de Janeiro, RJ, Brazil*

²*Departamento de Física, Universidade Federal Rural do Rio de Janeiro, 23897-000, Seropédica, RJ, Brazil*

³*Department of Physics, University of Michigan,
450 Church St, Ann Arbor, MI 48109-1040, USA and*

⁴*Faculdade de Tecnologia, Universidade do Estado do Rio de Janeiro, 27537-000, Resende, RJ, Brazil*

(Dated: September 15, 2023)

In standard cosmology, the cosmic homogeneity scale is the transition scale above which the patterns arising from non-uniformities – such as groups and clusters of galaxies, voids, and filaments – become indistinguishable from a random distribution of sources. Recently, different groups have investigated the feasibility of using such a scale as a cosmological test and arrived at different conclusions. In this paper, we complement and extend these studies by exploring the evolution of the spatial (\mathcal{R}_H) and angular (θ_H) homogeneity scales with redshift, assuming a spatially flat, Λ -Cold Dark Matter universe and linear cosmological perturbation theory. We confirm previous results concerning the non-monotonicity of \mathcal{R}_H with the matter density parameter Ω_{m0} but also show that it exhibits a monotonical behavior with the Hubble constant H_0 within a large redshift interval. More importantly, we find that, for $z \gtrsim 0.6$, the angular homogeneity scale not only presents a monotonical behavior with Ω_{m0} and H_0 but is quite sensitive to H_0 , especially at higher redshifts. These results, therefore, raise the possibility of using θ_H as a new, model-independent way to constrain cosmological parameters.

I. INTRODUCTION

The flat Λ -Cold Dark Matter (Λ CDM) model, where Λ represents the cosmological constant, has been established as the standard cosmological model (SCM) for over two decades. Although this model is able to provide a successful explanation to a variety of cosmological observations [1–6], it is plagued with several theoretical caveats, e.g. coincidence and fine-tuning problems [7], in addition to recent observational issues, such as the $\sim 5\sigma$ tension between early and late-time measurements of the Hubble constant (see e.g. [8] and references therein).

In light of these issues, it is paramount to test the foundations of the SCM, since any significant departure from their assumptions would require a complete reformulation of such paradigm. One of these hypothesis is the Cosmological Principle (CP), which states that the Universe looks statistically homogeneous and isotropic at sufficiently large scales, although lumpy and inhomogeneous at smaller scales due to the presence of cosmic structures like clusters, voids and filaments. Therefore, we can describe cosmological distances and ages by means of the Friedmann-Lemaître-Robertson-Walker (FLRW) metric from such scale onwards, as in the case of the SCM. Nonetheless, it should be stressed that we can only directly test the assumption of statistical isotropy,

not the homogeneity one. This happens because we are only able to observe cosmic sources on the intersection between our past light cone and the time-constant spatial hypersurfaces where they are located - hence, we can only perform consistency tests of this latter assumption. See [9–11] for a broad discussion on this topic.

Given the advent of large redshift surveys, numerous tests were carried out in order to measure the cosmic scale where the Universe appears consistent with the CP, i.e., the scale where the actual three-dimensional (3D) distribution of cosmic sources becomes statistically indistinguishable from a random one. Most of these tests could identify and measure such a characteristic scale, namely the cosmic homogeneity scale, \mathcal{R}_H , at around 70 – 150 Mpc using a variety of galaxy and quasar catalogues from these redshift surveys [12–22], albeit some works claimed otherwise [23–25], besides that these measurements could be biased by the survey window function [26].

Still, these measurements are only able to provide a consistency test of the SCM and the CP, as we need to convert the source redshifts into distances - and hence an assumption of a fiducial cosmological model must be made. This issue can be circumvented by using the angular homogeneity scale, θ_H , i.e., the two-dimensional (2D) measure of the homogeneity scale, given only in terms of the source position in the sky. This analysis was originally proposed by [27], being subsequently performed by [28–30] using different redshift survey catalogues.

Recently, it was proposed that the 3D homogeneity scale could be used as a sort of standard ruler, in a similar fashion to the sound horizon scale in baryonic acoustic oscillations measurements. Hence, it would be feasible to test cosmological models and constrain their parameters

*Electronic address: xiaoyun48@on.br

†Electronic address: rsousa@on.br

‡Electronic address: carlosbengaly@on.br

§Electronic address: uendsa@umich.edu

¶Electronic address: gabriela.coutinho@fat.uerj.br

**Electronic address: alcaniz@on.br

using \mathcal{R}_H measurements [31, 32]. However, a subsequent paper showed that such scale cannot provide a valid standard ruler, due to its nonmonotonic relation with the matter density parameter [33]. Still, it is worth mentioning that none of these works examined the feasibility of measurements of the angular (2D) homogeneity scale as a possible cosmological test.

The goal of this paper is to study the behavior of θ_H with redshift and investigate whether it can provide a one-to-one relation with respect to different values of cosmological parameters and the clustering bias, conversely from its three-dimensional counterpart, \mathcal{R}_H . Our analysis reveals that θ_H does exhibit a one-to-one correspondence with the matter density parameter (Ω_{m0}) and the Hubble constant (h) for $z \gtrsim 0.6$. Notably, we also found that this relationship is independent of the bias factor.

The structure of our paper is outlined as follows: Section II describes the theoretical framework of the homogeneity scale within the standard cosmological model paradigm. Section III presents the estimators and criteria commonly adopted to measure the homogeneity scale with observational data. Section IV is dedicated to the numerical outcomes of our analysis of the homogeneity scale, as described in the two previous sections. Finally, section V provides a summary of our study and the conclusions that we have drawn.

II. THEORETICAL FRAMEWORK

This section provides a brief description of our theoretical framework. Without loss of generality, we consider a spatially flat Λ CDM model as the underlying assumption.

The key quantity to be defined as an estimator for the angular cosmic homogeneity scale consists on the fractal dimension, $\mathcal{D}_2(\theta)$. As originally proposed in [27], and adapted in [29, 30], $\mathcal{D}_2(\theta)$ can be described in terms of the 2-point angular correlation function (2PACF) of a galaxy catalogue, which reads:

$$\mathcal{D}_2(\theta) = 2 + \frac{d \ln}{d \ln \theta} \left[1 + \frac{1}{1 - \cos \theta} \int_0^\theta \omega(\theta') \sin \theta' d\theta' \right], \quad (1)$$

where $\omega(\theta')$ represents the 2PACF, defined as the excess probability of finding pairs of galaxies - or any kind of dark matter tracers - compared to a random Poisson distribution, and θ denotes the angular separation on the sky between the pairs.

As for the 2PACF, it can be expressed as [34]

$$w(\theta) = \int dz_1 f(z_1) \int dz_2 f(z_2) \xi(r(z_1), r(z_2), \theta, \bar{z}) \quad (2)$$

where ξ is the matter three-dimensional two-point correlation function, and we assume $f(z) \equiv b(z)\phi(z)$, with $b(z)$ being the bias parameter and $\phi(z)$ the radial selection, which is the probability to include a galaxy in a

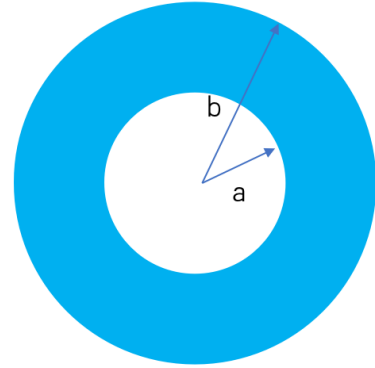


FIG. 1: An illustration of the two-dimensional shell where the 2PACF is computed.

given redshift bin. The comoving distance to redshift z is given by

$$r(z) = \int_0^z \frac{c}{H(z')} dz' \quad (3)$$

where

$$H(z) = H_0 \sqrt{\Omega_m(1+z)^3 + (1 - \Omega_m)}. \quad (4)$$

Note that we will hereafter refer to the Hubble Constant as a dimensionless quantity, defined as $h \equiv H_0/(100 \text{ km s}^{-1} \text{ Mpc}^{-1})$.

In this paper, we will compute the 2PACF by integrating the comoving distance using the Limber approximation [35], as in [36][37]:

$$w(\theta) \approx \int_0^\infty dr_1 \int_0^\infty dr_2 P_1(r_1) P_2(r_2) \xi(R), \quad (5)$$

where

$$R \equiv \sqrt{r_1^2 + r_2^2 - 2r_1 r_2 \cos \theta} \quad (6)$$

and $P_1(r_1)$, $P_2(r_2)$ correspond to the comoving radial distance distribution of the sample. The approximation made by Limber consists on assuming that the width of the functions P_1 and P_2 is much greater than the correlation length of $\xi(R)$ [38]. Since we only consider top-hat window functions and narrow redshift bins, these quantities can be expressed by

$$P_1 = P_2 = P(r) \approx \begin{cases} 0 & 0 \leq r < a \\ \frac{1}{b-a} & a \leq r < b \\ 0 & r \geq b \end{cases} \quad (7)$$

where a and b are the inner and outer radius, respectively, of the spherical shell where the 2PACF is computed, as shown in Figure 1.

On the other hand, the 3D two-point correlation function $\xi(r)$ can be expressed by

$$\xi(r) = \frac{1}{2\pi^2} \int_0^\infty j_0(kr) k^2 P(k) dk, \quad (8)$$

where the matter power spectrum, denoted as $P(k)$, is related to the spherical Bessel function $j_0(x)$, i.e., $j_0(x) = \frac{\sin(x)}{x}$. In this work, our focus is solely on large cosmological scales, thus restricting our analysis to the linear segment of the spectrum. Hence, we can assume the linear perturbation theory and, for simplicity, we disregard redshift-space distortions (RSDs) in the \mathcal{D}_2 calculation.

III. METHOD AND ESTIMATORS

In order to obtain an observational measurement of the cosmic homogeneity scale using the fractal dimension \mathcal{D}_2 , firstly we must define the integral correlation \mathcal{N} . This quantity can be expressed in terms of the scaled count-in-spheres, which consists on the number of neighboring galaxies in a 2D-sphere of radius θ around a given data point, $N(<\theta)$, compared to the average number of neighboring galaxies around a data point in a synthetic random catalogue - but still at the same angular scale θ - as denoted by $N_{\text{random}}(<\theta)$. Hence, we can write the integral correlation as

$$\mathcal{N}(<\theta) = \frac{N(<\theta)}{N_{\text{random}}(<\theta)}, \quad (9)$$

where the term in the denominator is used to account for geometric effects [14].

Assuming a spatially flat universe, the number of objects will scale as $N_{\text{random}}(<\theta) \propto \theta^2$ for small angle θ - implicitly assuming that the observational catalogue is properly complete, homogeneous and clean of possible impurities e.g. stellar contamination - while in general the number of objects in a real catalogue will scale as $N(<\theta) \propto \theta^{\mathcal{D}_2}$. Thus, the determination of the fractal dimension \mathcal{D}_2 involves the utilisation of the logarithmic derivative of the integral correlation

$$\mathcal{D}_2(\theta) = 2 + \frac{d \ln \mathcal{N}(<\theta)}{d \ln \theta}. \quad (10)$$

In practice, the integral correlation can be associated to the 2PACF - see the second term in the right-hand side of Eq. (1). For a broader discussion on this topic, we refer the reader to [29].

The value of the fractal dimension should asymptotically approach the number of environmental dimensions at scales where the underlying distribution becomes statistically homogeneous. In other words, we should expect that

$$\mathcal{D}_2(\theta) \rightarrow 2 \quad \text{for } \theta \rightarrow \theta_H, \quad \forall \theta \leq 20^\circ. \quad (11)$$

In this work, we also assume that the angular homogeneity scale is reached where \mathcal{D}_2 approaches 1% of its expected value, following [14]. This implies that θ_H represents the angular scale where

$$\mathcal{D}_2(\theta_H) = 1.98. \quad (12)$$

Therefore, we can obtain a theoretical prediction of θ_H as the angular scale where the fractal dimension \mathcal{D}_2 , as defined in Eq. (1), satisfies the condition shown above for a given set of cosmological parameters. This is how we will carry out our numerical work, as we shall present in the following sections.

Before proceeding further, it is worth mentioning that authors of Ref. [33] showed that the 3D homogeneity scale, i.e., the value of \mathcal{R}_H where $\mathcal{D}_2^{3d} = 2.97$ could not be a feasible standard ruler, as it does not show a one-to-one relation with the matter density parameter Ω_{m0} in the Λ CDM model - in the paper, it is unclear at which redshift the calculations were performed. Moreover, the feasibility of measurements of the angular homogeneity scale θ_H as a cosmological was not investigated. Thus, in what follows, we extend the previous analysis to various redshifts, clustering bias, and cosmological parameter values within the standard model, particularly emphasizing the angular homogeneity scale case.

IV. NUMERICAL RESULTS

A. Spatial homogeneity scale

Firstly, we compute the theoretical predictions of the three-dimensional (spatial) homogeneity scales, by the same token of [33]. Figure 2 shows the galaxy two point correlation function, denoted as $\xi(r)$ (left), and the fractal dimension $\mathcal{D}_2(r)$ (right) at $z = 0.4$. We assumed Ω_{m0} values within the range $[0.15, 0.8]$, as depicted in each coloured line of both panels¹. The dashed line corresponds to the $\mathcal{D}_2 = 2.97$ condition, where the cosmic three-dimensional scale R can be assigned as \mathcal{R}_H , as discussed in section III.

Fig. 3 displays the homogeneity scale \mathcal{R}_H as a function of the dimensionless Hubble constant h (left panel), whose range is $h = [0.4, 1.0]$, and of the present-day matter density Ω_{m0} (right panel). All plots assume a clustering bias value of $b = 1.5$. We can see that \mathcal{R}_H exhibits a one-to-one, monotonically increasing function for all values of h assumed, but it indeed exhibits a non-monotonically behaviour for $\Omega_{m0} = [0.15, 0.8]$ values. Hence, our first numerical results on Ω_{m0} agree with those shown in [33]. Moreover, we present numerical results for the same quantities (ξ , \mathcal{D}_2 , and \mathcal{R}_H) for two arbitrary redshift values, i.e., $z = 0.64$ and $z = 3.0$, as displayed in Figs. 8 and 9 and Figs. 10 and 11 of the Appendix A, respectively. For the same intervals of $h = [0.4, 1.0]$ and $\Omega_{m0} = [0.15, 0.8]$, we find that the \mathcal{R}_H is a one-to-one function for different values of h , but not for Ω_{m0} . Therefore, our results confirm that the scale of cosmic homogeneity cannot be used alone as a cosmolog-

¹ Note that we change the value of Ω_{m0} by keeping Ω_{b0} constant and varying Ω_{c0} .

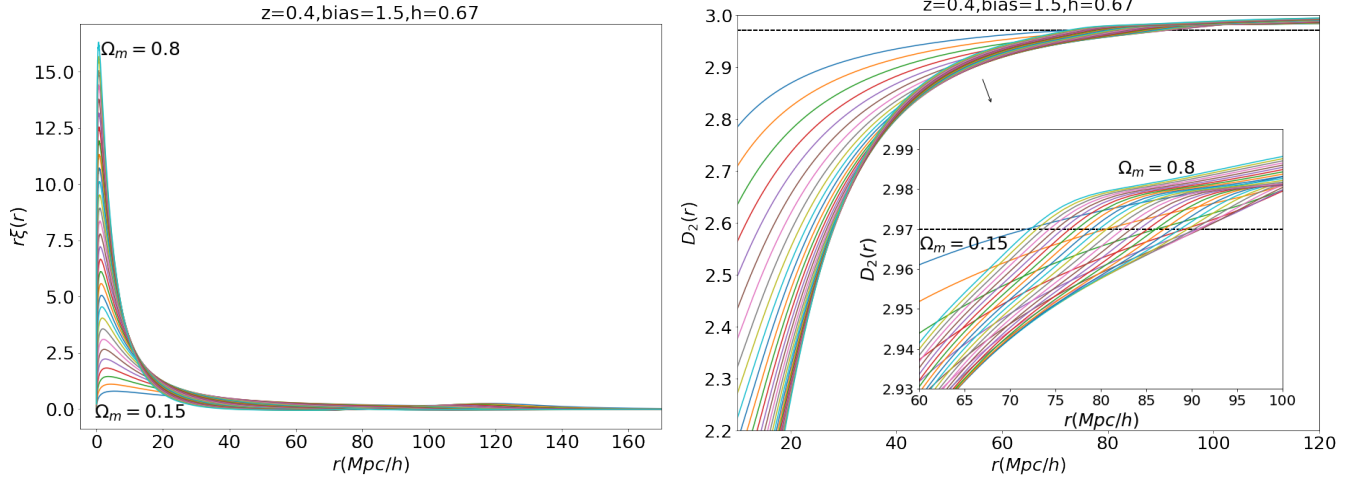


FIG. 2: The 2PCF $\xi(r)$ (left) and the fractal dimension $\mathcal{D}_2(r)$ (right) for $\Omega_{m0} \in [0.15, 0.8]$ at $z = 0.4$. In the right panel, the dashed line corresponds to 1% deviation from homogeneity.

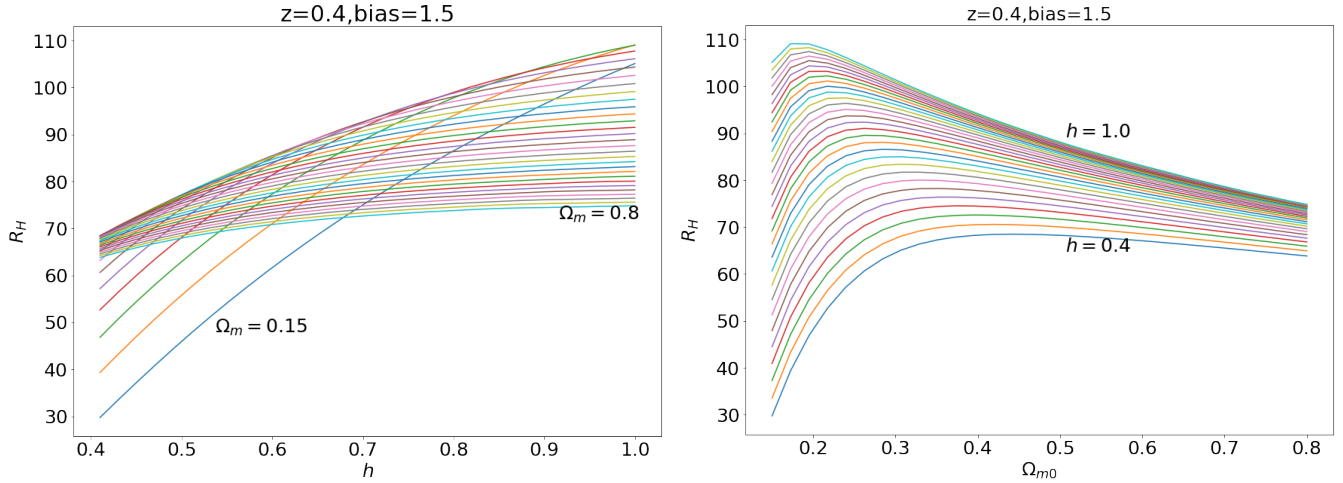


FIG. 3: The homogeneity scale R_H as a function of the hubble constant h for $\Omega_{m0} \in [0.15, 0.8]$ (left) and of the present-day matter density Ω_{m0} for $h \in [0.4, 1.0]$ (right) at $z = 0.4$. The homogeneity scale R_H exhibits a monotonically increasing behavior for all values of h and a non-monotonically behavior for Ω_{m0} in the range considered.

ical probe to measure cosmological parameters such as Ω_{m0} .

As for additional remarks, we show that the homogeneity scale R_H only exhibits small change with respect to reasonable values of Ω_{m0} , i.e., from 0.21 to 0.41, at different redshift ranges. We see a $\sim 3\%$, $\sim 3\%$, $\sim 15\%$ relative change at redshift $z = 0.4$, 0.64 , and 3.0 , respectively, for Ω_{m0} within this range. On the other hand, the homogeneity scale R_H significantly changes with respect to h values from 0.6 to 0.8 - roughly $\sim 6.7\%$, $\sim 8.6\%$, and $\sim 16.1\%$ at those same redshift values, respectively.

B. Angular homogeneity scale

Following the same token of the spatial homogeneity scale analysis, we display in Fig. 4 the angular correlation function of galaxies ($\omega(\theta)$) in the left panel, and the fractal dimension ($\mathcal{D}_2(\theta)$) in the right panel, for a redshift value of $z = 0.4$, and for a range of values of the matter density parameter Ω_{m0} within the interval of $[0.15, 0.8]$. In Fig. 5, we present the homogeneity scale θ_H as a function of the Hubble constant h (also within the range $h = [0.4, 1.0]$), and as a function of the present-day matter Ω_{m0} in the left and right panels, respectively. The dashed line corresponds to a deviation of 1% from angular homogeneity. Our results show that the function θ_H does exhibit monotonicity concerning the range of h assumed, but θ_H does not exhibit a one-to-one correspon-

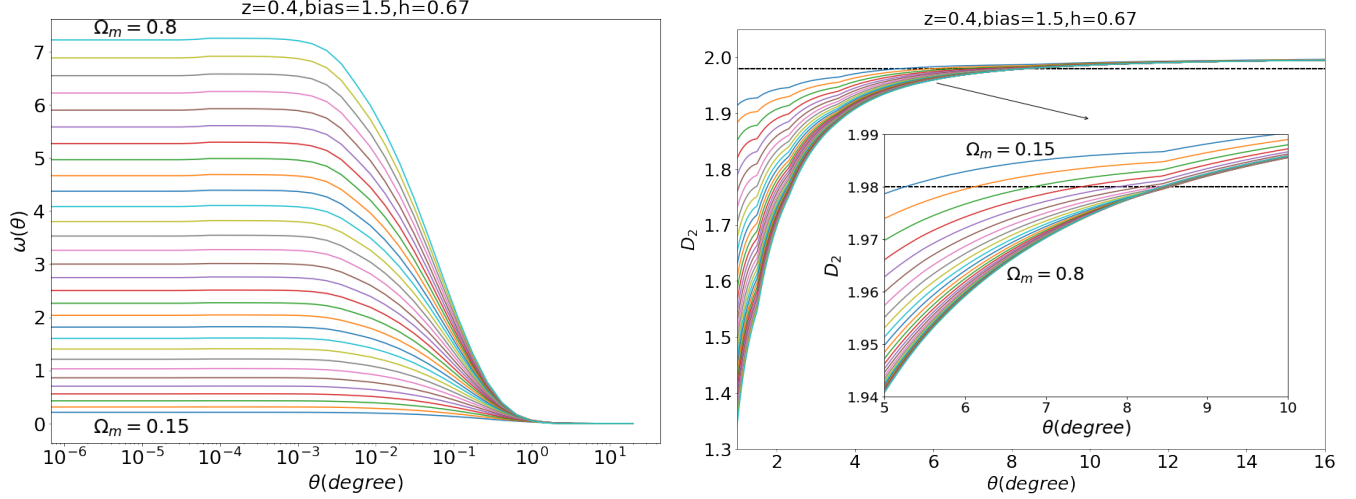


FIG. 4: The 2PACF $\omega(\theta)$ (left) and the fractal dimension $\mathcal{D}_2(\theta)$ (right) for $\Omega_{m0} \in [0.15, 0.8]$ at $z = 0.4$. The dashed line corresponds to 1% deviation from angular homogeneity.

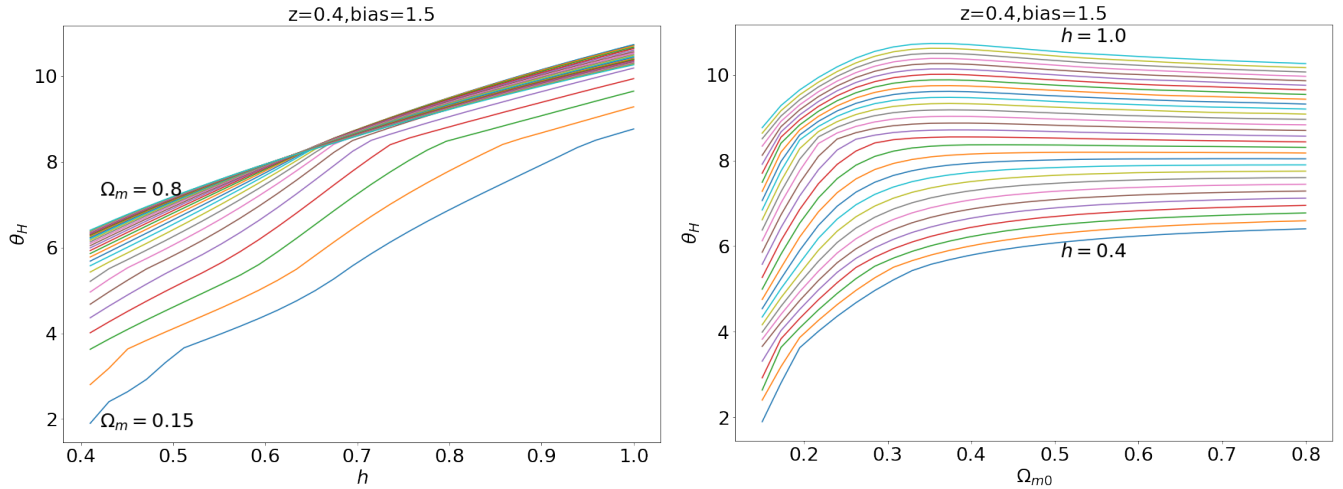


FIG. 5: The angular homogeneity scale θ_H as a function of the Hubble constant h for $\Omega_{m0} \in [0.15, 0.8]$ (left) and of present-day matter density Ω_{m0} for $h \in [0.4, 1.0]$ (right) at $z = 0.4$. Clearly, θ_H is a monotonically increasing function for all values of h but exhibits a different behavior for Ω_{m0} , similarly to the \mathcal{R}_H case.

dence for the Ω_{m0} values within the specified interval and redshift.

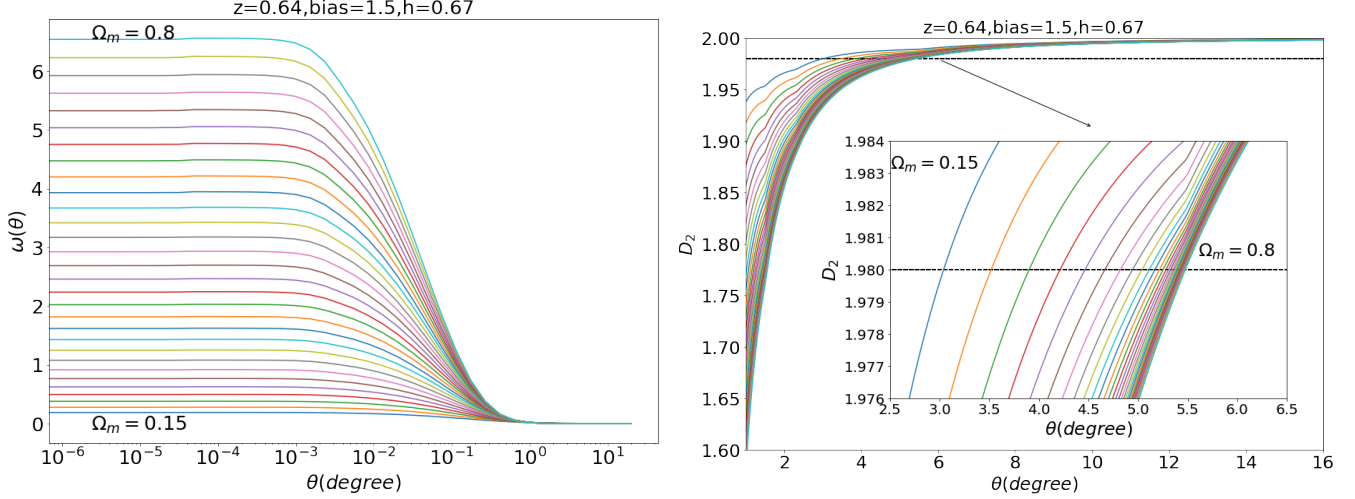
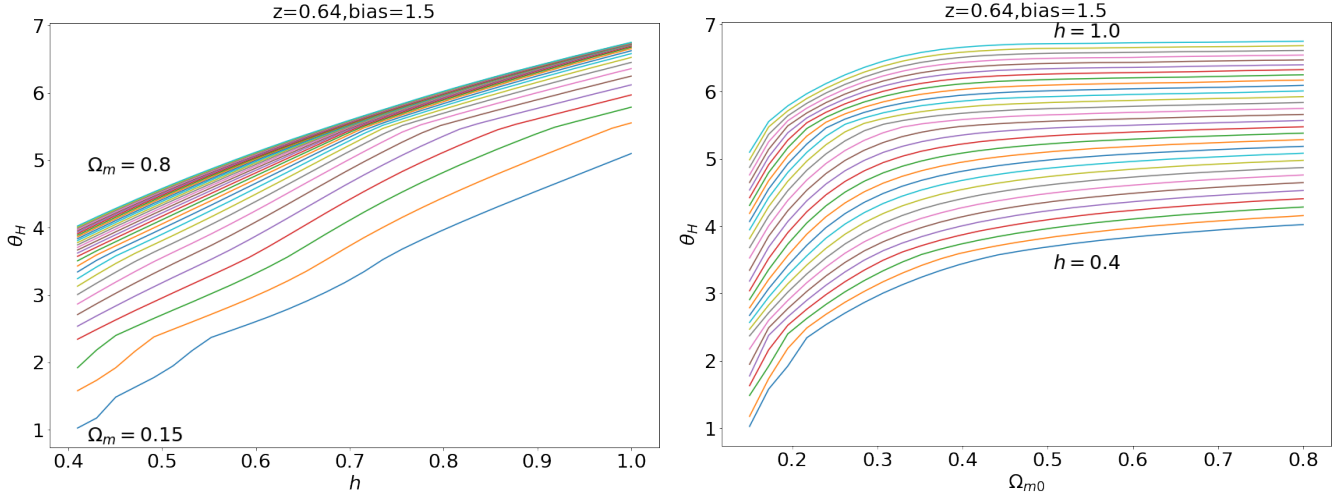
Nonetheless, we should remark that this behaviour changes for higher redshift ranges. For $z = 0.64$, for instance, our numerical results for $\omega(\theta)$ and $\mathcal{D}_2(\theta)$ (left and right panels in Fig. 6, respectively), as well as for θ_H as a function of h and Ω_m (left and right panels in Fig. 7, respectively), indicate that the angular homogeneity scale θ_H does exhibit a one-to-one correspondence with Ω_{m0} ranging from 0.15 to 0.8, conversely from its 3D counterpart. Hence, our result demonstrates that θ_H can be used as a feasible cosmological test for both Ω_m and h parameters, given that the redshift is high enough to break the non-monotonicity between Ω_{m0} and θ_H . A similar behaviour is found for the $z = 3.0$ case, as exhibited in Figures 12 and 13 (Appendix A). We emphasize that all

results shown above were obtained by fixing the clustering bias to $b = 1.5$. However, we also performed analyses with other values for the bias parameter, and our conclusions were unchanged.

V. CONCLUSIONS

In this paper, we revisited, complemented and extended the discussion about the feasibility of measurements of the homogeneity scale as a cosmological test. Assuming a spatially flat Λ CDM model, we conducted a comparative analysis of the behavior of both spatial (\mathcal{R}_H) and angular (θ_H) homogeneity scales as a function of the redshift.

In agreement with [33], our first results showed that

FIG. 6: The same as Fig. 4, for $z = 0.64$.FIG. 7: The same as Fig. 5, for $z = 0.64$. Conversely from this case, we find that the angular homogeneity scale θ_H is indeed a one-to-one function for both h and Ω_{m0} in the interval considered.

the spatial homogeneity scales do not exhibit a one-to-one behavior for reasonable values of Ω_{m0} , as estimated by current observations. However, they also showed a monotonical behavior of \mathcal{R}_H for reasonable values of the Hubble constant within a large redshift interval. Actually, \mathcal{R}_H was found to be significantly influenced by h , with a variation of $\sim 6.7\%$, $\sim 8.6\%$, and $\sim 16.0\%$ at redshifts of 0.4, 0.64, and 3.0, respectively.

On the other hand, for $z \gtrsim 0.6$, we showed that the angular homogeneity scale is not only a one-to-one function for reasonable intervals of Ω_{m0} and h , but it is also quite sensitive to values of h , varying by $\sim 13.2\%$, $\sim 15.1\%$, and $\sim 18.5\%$ at redshifts 0.4, 0.64, and 3.0, respectively. Compared to \mathcal{R}_H , the sensitivity of the θ_H to reasonable values of Ω_{m0} also increases.

Finally, it is important to mention that θ_H is obtained in a model-independent way, differently from its 3D coun-

terpart \mathcal{R}_H . Therefore, the results of this paper showing the one-to-one behavior of θ_H with Ω_{m0} and h for intermediate and high redshifts are also crucial to ensure a new, model-independent way to estimate cosmological parameters. This kind of observable is particularly important given the current tensions of the standard cosmology and the many alternatives to solve them. An application of the $\theta_H(z)$ test is currently underway, and its results will appear in a forthcoming communication.

Acknowledgements

XS acknowledges financial support through a PhD fellowship from the Coordenação de Aperfeiçoamento de Pessoal de Nível Superior (CAPES). CB acknowledges financial support from Fundação Carlos Chagas Filho

de Amparo à Pesquisa do Estado do Rio de Janeiro (FAPERJ) - Postdoc Nota 10 fellowship. UA has been supported by Department of Energy under contract DE-FG02-95ER40899, and Leinweber Center for Theoretical

Physics at the University of Michigan. JSA is supported by Conselho Nacional de Desenvolvimento Científico e Tecnológico (CNPq 307683/2022-2) and FAPERJ grant 259610 (2021).

-
- [1] N Aghanim, Y Akrami, M Ashdown, J Aumont, C Bacigalupi, M Ballardini, AJ Banday, RB Barreiro, N Bartolo, S Basak, et al. Planck 2018 results-vi. cosmological parameters (corrigendum). *Astronomy & Astrophysics*, 652:C4, 2021.
 - [2] Dillon Brout et al. The Pantheon+ Analysis: Cosmological Constraints. *Astrophys. J.*, 938(2):110, 2022.
 - [3] Shadab Alam et al. Completed SDSS-IV extended Baryon Oscillation Spectroscopic Survey: Cosmological implications from two decades of spectroscopic surveys at the Apache Point Observatory. *Phys. Rev. D*, 103(8):083533, 2021.
 - [4] T. M. C. Abbott et al. Dark Energy Survey Year 3 results: Cosmological constraints from galaxy clustering and weak lensing. *Phys. Rev. D*, 105(2):023520, 2022.
 - [5] Mathew S. Madhavacheril et al. The Atacama Cosmology Telescope: DR6 Gravitational Lensing Map and Cosmological Parameters. 4 2023.
 - [6] Xiangchong Li et al. Hyper Suprime-Cam Year 3 Results: Cosmology from Cosmic Shear Two-point Correlation Functions. 4 2023.
 - [7] Steven Weinberg. The Cosmological constant problems. In *4th International Symposium on Sources and Detection of Dark Matter in the Universe (DM 2000)*, pages 18–26, 2 2000.
 - [8] Eleonora Di Valentino, Olga Mena, Supriya Pan, Luca Visinelli, Weiqiang Yang, Alessandro Melchiorri, David F. Mota, Adam G. Riess, and Joseph Silk. In the realm of the Hubble tension—a review of solutions. *Class. Quant. Grav.*, 38(15):153001, 2021.
 - [9] Chris Clarkson and Roy Maartens. Inhomogeneity and the foundations of concordance cosmology. *Class. Quant. Grav.*, 27:124008, 2010.
 - [10] Roy Maartens. Is the Universe homogeneous? *Phil. Trans. Roy. Soc. Lond. A*, 369:5115–5137, 2011.
 - [11] Chris Clarkson. Establishing homogeneity of the universe in the shadow of dark energy. *Comptes Rendus Physique*, 13:682–718, 2012.
 - [12] David W. Hogg, Daniel J. Eisenstein, Michael R. Blanton, Neta A. Bahcall, J. Brinkmann, James E. Gunn, and Donald P. Schneider. Cosmic homogeneity demonstrated with luminous red galaxies. *Astrophys. J.*, 624:54–58, 2005.
 - [13] Prakash Sarkar, Jaswant Yadav, Biswajit Pandey, and Somnath Bharadwaj. The scale of homogeneity of the galaxy distribution in SDSS DR6. *Mon. Not. Roy. Astron. Soc.*, 399:L128–L131, 2009.
 - [14] Morag Scrimgeour et al. The WiggleZ Dark Energy Survey: the transition to large-scale cosmic homogeneity. *Mon. Not. Roy. Astron. Soc.*, 425:116–134, 2012.
 - [15] Biswajit Pandey. A method for testing the cosmic homogeneity with Shannon entropy. *Mon. Not. Roy. Astron. Soc.*, 430:3376, 2013.
 - [16] Biswajit Pandey and Suman Sarkar. Testing homogeneity in the Sloan Digital Sky Survey Data Release Twelve with Shannon entropy. *Mon. Not. Roy. Astron. Soc.*, 454(3):2647–2656, 2015.
 - [17] Suman Sarkar and Biswajit Pandey. An information theory based search for homogeneity on the largest accessible scale. *Mon. Not. Roy. Astron. Soc.*, 463(1):L12–L16, 2016.
 - [18] Pierre Laurent et al. A $14 h^{-3} \text{ Gpc}^3$ study of cosmic homogeneity using BOSS DR12 quasar sample. *JCAP*, 11:060, 2016.
 - [19] Pierros Ntelis et al. Exploring cosmic homogeneity with the BOSS DR12 galaxy sample. *JCAP*, 06:019, 2017.
 - [20] R. S. Gonçalves, G. C. Carvalho, C. A. P. Bengaly, J. C. Carvalho, and J. S. Alcaniz. Measuring the scale of cosmic homogeneity with SDSS-IV DR14 quasars. *Mon. Not. Roy. Astron. Soc.*, 481(4):5270–5274, 2018.
 - [21] Rodrigo S. Gonçalves, Gabriela C. Carvalho, Uendert Andrade, Carlos A. P. Bengaly, Joel C. Carvalho, and Jailson Alcaniz. Measuring the cosmic homogeneity scale with SDSS-IV DR16 Quasars. *JCAP*, 03:029, 2021.
 - [22] Yigon Kim, Chan-Gyung Park, Hyerim Noh, and Jai-chan Hwang. CMASS galaxy sample and the ontological status of the cosmological principle. *Astron. Astrophys.*, 660:A139, 2022.
 - [23] Francesco Sylos Labini, Nikolay L. Vasilyev, Yuriy V. Baryshev, and Martin Lopez-Corredoira. Absence of anti-correlations and of baryon acoustic oscillations in the galaxy correlation function from the Sloan Digital Sky Survey DR7. *Astron. Astrophys.*, 505:981–990, 2009.
 - [24] Francesco Sylos Labini. Very large scale correlations in the galaxy distribution. *EPL*, 96(5):59001, 2011.
 - [25] Chan-Gyung Park, Hwasu Hyun, Hyerim Noh, and Jai-chan Hwang. The cosmological principle is not in the sky. *Mon. Not. Roy. Astron. Soc.*, 469(2):1924–1931, 2017.
 - [26] Asta Heinesen. Cosmological homogeneity scale estimates are dressed. *JCAP*, 10:052, 2020.
 - [27] D. Alonso, A. Bueno belloso, F. J. Sánchez, J. García-Bellido, and E. Sánchez. Measuring the transition to homogeneity with photometric redshift surveys. *Mon. Not. Roy. Astron. Soc.*, 440(1):10–23, 2014.
 - [28] David Alonso, Ana Isabel Salvador, Francisco Javier Sánchez, Maciej Bilicki, Juan García-Bellido, and Eusebio Sánchez. Homogeneity and isotropy in the Two Micron All Sky Survey Photometric Redshift catalogue. *Mon. Not. Roy. Astron. Soc.*, 449(1):670–684, 2015.
 - [29] R. S. Gonçalves, G. C. Carvalho, C. A. P. Bengaly, J. C. Carvalho, A. Bernui, J. S. Alcaniz, and R. Maartens. Cosmic homogeneity: a spectroscopic and model-independent measurement. *Mon. Not. Roy. Astron. Soc.*, 475(1):L20–L24, 2018.
 - [30] Uendert Andrade, Rodrigo S. Gonçalves, Gabriela C. Carvalho, Carlos A. P. Bengaly, Joel C. Carvalho, and Jailson Alcaniz. The angular scale of homogeneity with SDSS-IV DR16 luminous red galaxies. *JCAP*, 10:088, 2022.
 - [31] Pierros Ntelis, Anne Ealet, Stephanie Escoffier, Jean-

- Christophe Hamilton, Adam James Hawken, Jean-Marc Le Goff, James Rich, and Andre Tilquin. The scale of cosmic homogeneity as a standard ruler. *JCAP*, 12:014, 2018.
- [32] Pierros Ntelis, Adam James Hawken, Stephanie Escoffier, Anne Ealet, and Andre Tilquin. Cosmological constraints from cosmic homogeneity. 4 2019.
- [33] Savvas Nesseris and Manuel Trashorras. Can the homogeneity scale be used as a standard ruler? *Phys. Rev. D*, 99(6):063539, 2019.
- [34] Martín Crocce, Anna Cabré, and Enrique Gaztanaga. Modelling the angular correlation function and its full covariance in photometric galaxy surveys. *Monthly Notices of the Royal Astronomical Society*, 414(1):329–349, 2011.
- [35] D. Nelson Limber. The Analysis of Counts of the Extragalactic Nebulae in Terms of a Fluctuating Density Field. *Astrophys. J.*, 117:134, January 1953.
- [36] Patrick Simon. How accurate is limber’s equation? *Astronomy & Astrophysics*, 473(3):711–714, 2007.
- [37] Xiaoyun Shao, Zhoujian Cao, Xilong Fan, and Shichao Wu. Probing the large-scale structure of the universe through gravitational wave observations. *Research in Astronomy and Astrophysics*, 22(1):015006, 2022.
- [38] Harold Francke. Clustering of lyman-alpha emitters galaxies. *New Astronomy Reviews*, 53(3):47–49, 2009.

Appendix

1. Additional results for higher redshifts

For completeness, we present below numerical results for the quantities ξ , ω , \mathcal{D}_2 , R_H and θ_H for $z = 0.64$ and $z = 3.0$.

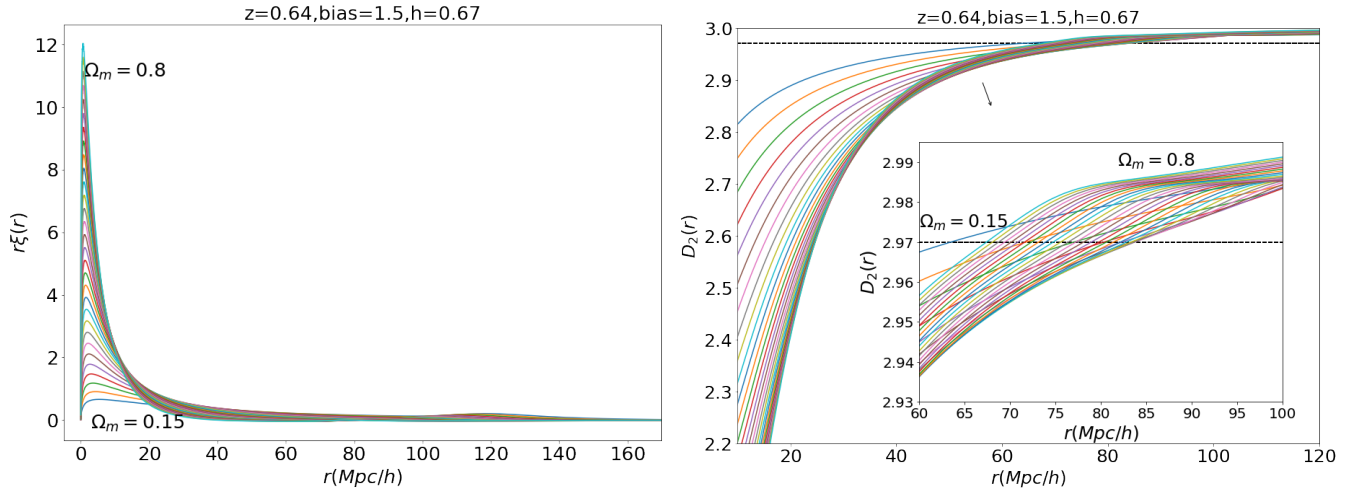
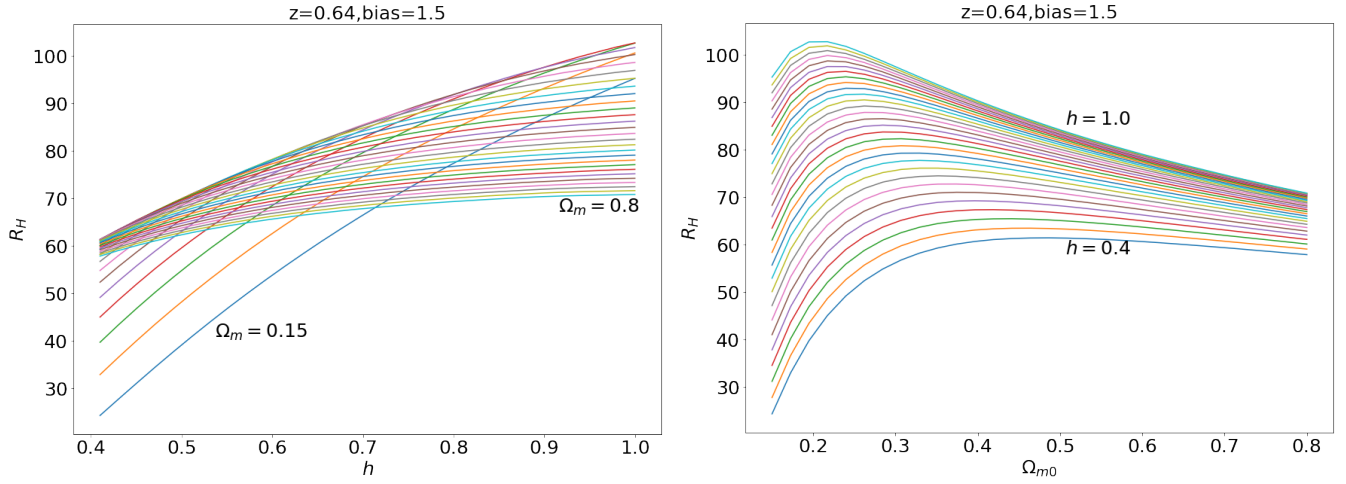
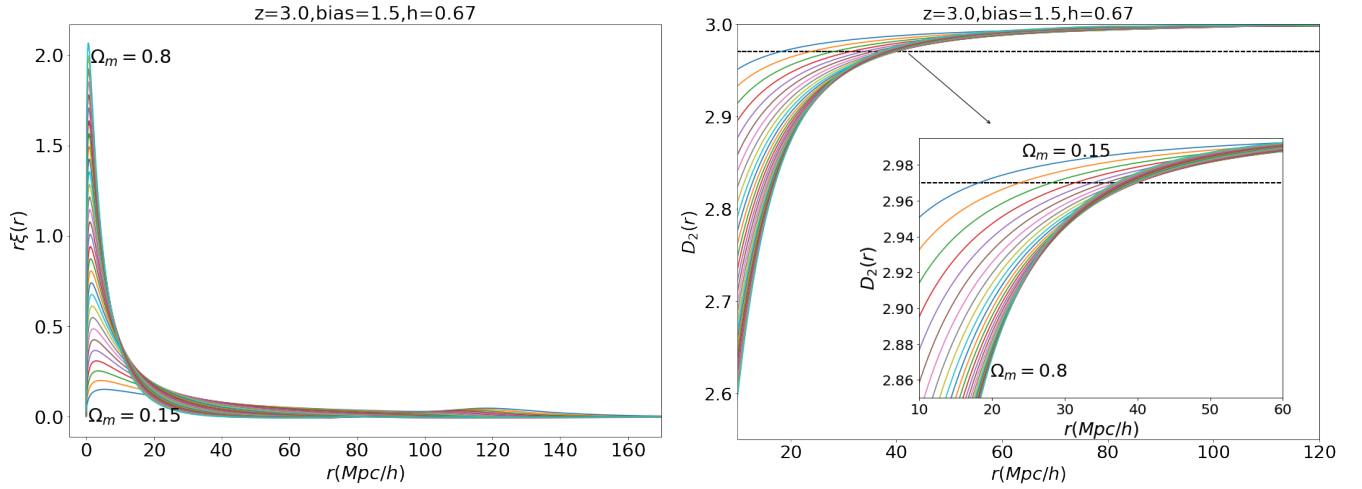
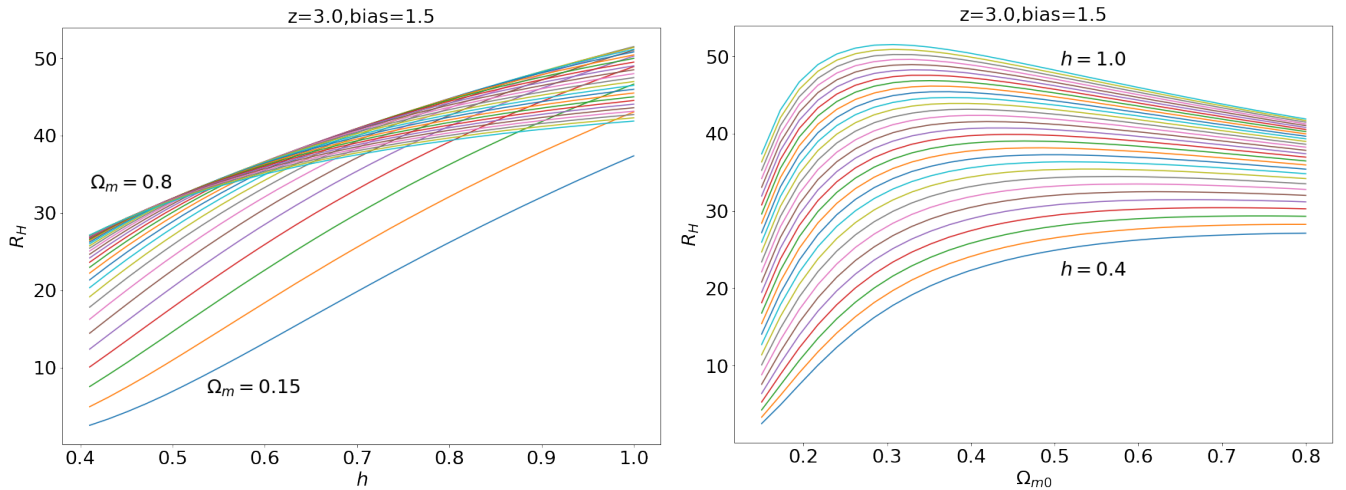
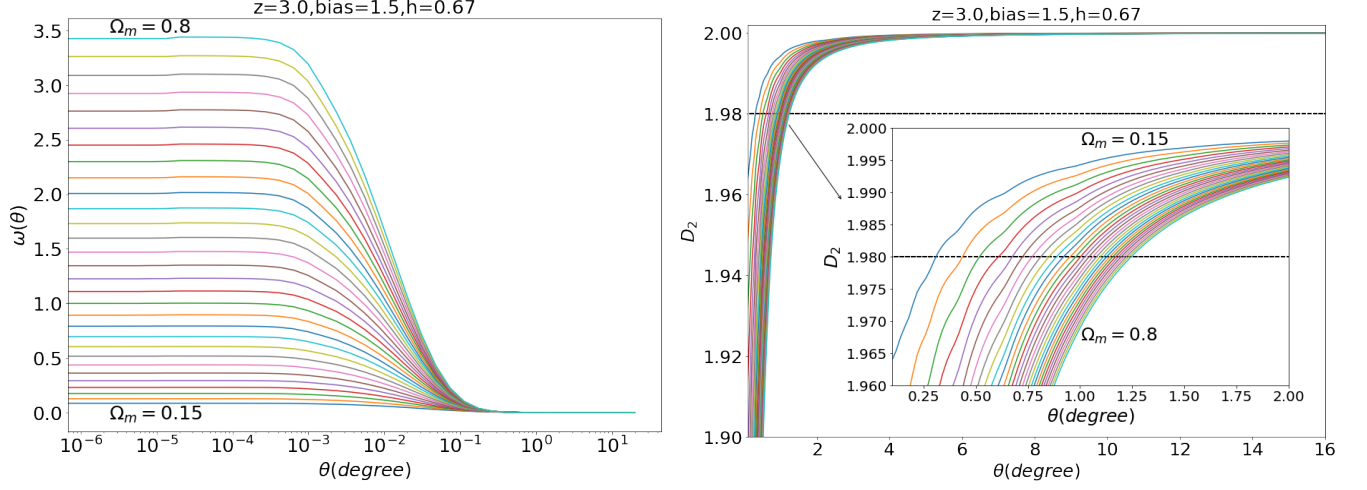
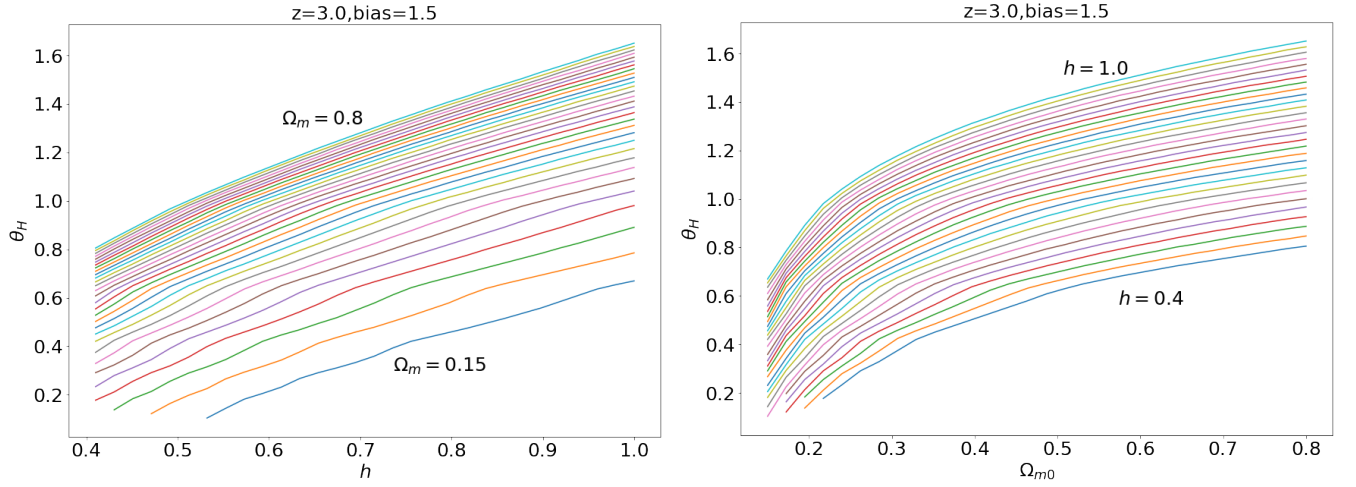


FIG. 8: The same as Fig. 2, for $z = 0.64$.

FIG. 9: The same as Fig. 3, for $z = 0.64$.FIG. 10: The same as Fig. 2, for $z = 3.0$.FIG. 11: The same as Fig. 3, for $z = 3.0$.

FIG. 12: The same as Fig. 4, for $z = 3.0$.FIG. 13: The same as Fig. 5, but for $z = 3.0$. Conversely from this case, we find that the angular homogeneity scale θ_H is indeed a one-to-one function for both h and Ω_{m0} in those ranges, as for $z = 0.64$.